Graphene and Quantum Electrodynamics in $2+1$ Dimensions

V.P. Gusynin

Bogolyubov Institute for Theoretical Physics, Kiev, Ukraine

Summer School on Modern Quantum Technologies 2018, Kiev, Ukraine

September 10, 2018

Outline

- Introduction: Why graphene is so interesting?
- Dirac theory of graphene
- QED form of graphene Lagrangian
- Graphene in a magnetic field: Landau levels and Quantum Hall effect
- Supercritical Coulomb center: resonant states
- Dynamical mass generation in QFT
- Gap generation in graphene
- Other two-dimensional Dirac materials

Why graphene is so interesting?

- Atomic structure. Graphene is an one-atom-thick layer of graphite packed in the honeycomb lattice – a two-dimensional crystal. Free suspended graphene shows "rippling" of the flat sheet with amplitude of about one nanometer.
- The ability to sustain huge ($> 10^8 A/cm^2$) electric currents make it a promising candidate for applications in devices such as nanoscale field effect transistors.
- Graphene exhibits the highest electronic quality among all known materials. It has a high electron mobility at room temperature, $\mu \sim 15000 cm^2/V \cdot s$. In free suspended graphene $\mu \sim 150000 cm^2/V \cdot s$: the quasiparticles in graphene take less than 0.1 ps to cover the typical distance between source and drain electrods in a transistor.

Why graphene is so interesting?

- Easy control of charged carriers.
- Anomalous quantum Hall effect: $\sigma_{xy} = \pm 4(n + 1/2)\frac{e^2}{h}$.
- Thermal properties. The thermal conductivity $\kappa \sim 5 \cdot 10^3 W/m \cdot K$ is larger that for carbon nanotubes or diamond.
- Optical properties. Graphene has high optical transparency: it absorbs only $\pi\alpha \approx 2.3\%$ of white light ($\alpha = 1/137$ - fine structure constant). This can be important for making liquid crystal displays.
- Mechanical properties. Graphene is the strongest material ever tested, stiffness - $340 N/m$. Because of this graphene remains stable and conductive at extremely small scales of order several nanometers.

Graphene as a bench top QED

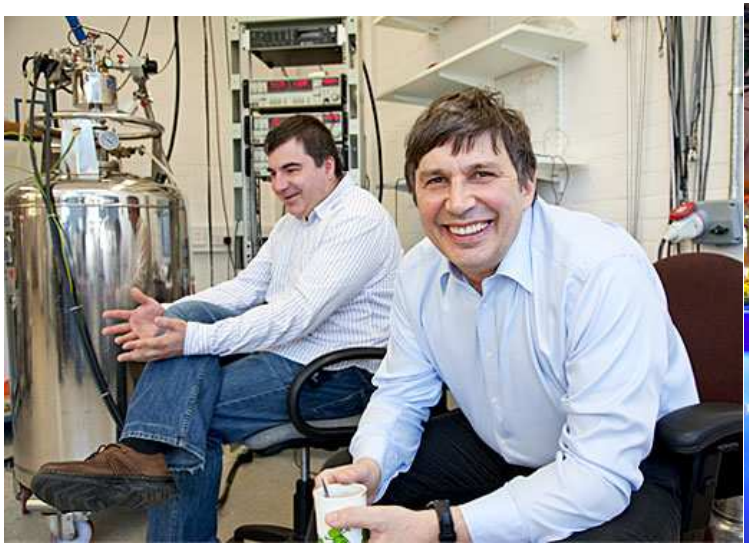

- the Klein tunneling (Young, Kim, Nature Physics, 2009)
- zitterbewegung (trembling motion)
- the Schwinger pair production
- the Casimir effect
- supercritical atomic collapse (Wang et al., Science, 2013)
- symmetry broken phase with a gap at strong coupling

Qusiparticle zoo

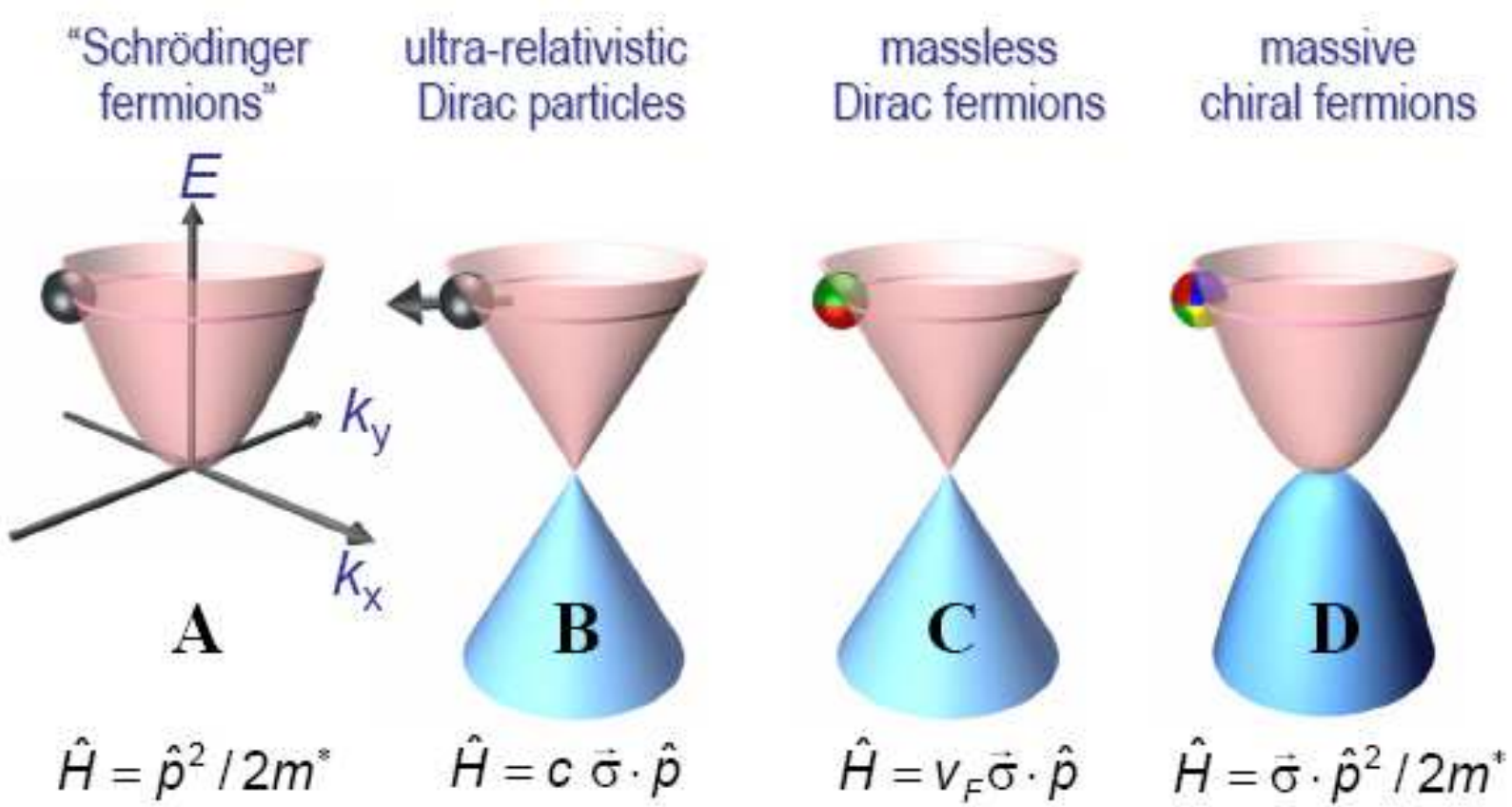

Reviews

- A.C. Neto, F. Guinea and N.M. Peres. Drawing conclusions from graphene. Physics World, 19, 33 (2006).
- M. Katsnelson, Graphene: carbon in two dimensions. Materials today, 10, 20 (2007).
- A.Geim and K. Novoselov. The rise of graphene. Nature Materials 6, 183 (2007).
- V.P. Gusynin, S.G. Sharapov, J.P. Carbotte. AC conductivity of graphene: from tight-binding model to 2+1-dimensional quantum electrodynamics. Int.J.Mod.Phys.B21, 4611-4658 (2007).
- A. H. Castro Neto, F. Guinea, N. M. R. Peres, K. S. Novoselov, A. K. Geim. The electronic properties of graphene. Rev. Mod. Phys. 81, 109 (2009).

One atomic layer of graphene

In 2004, the Manchester group (A. Geim, K. Novoselov et al.) obtained graphene by mechanical exfoliation of graphite. They used cohesive tape to repeatedly split graphite crystals into increasingly thinner pieces. This micromechanical "peeling" created flakes, some of which were – unexpectedly – just one layer thick. The key for the success was the use of a properly chosen substrate, which provides a small but noticeable optical contrast.

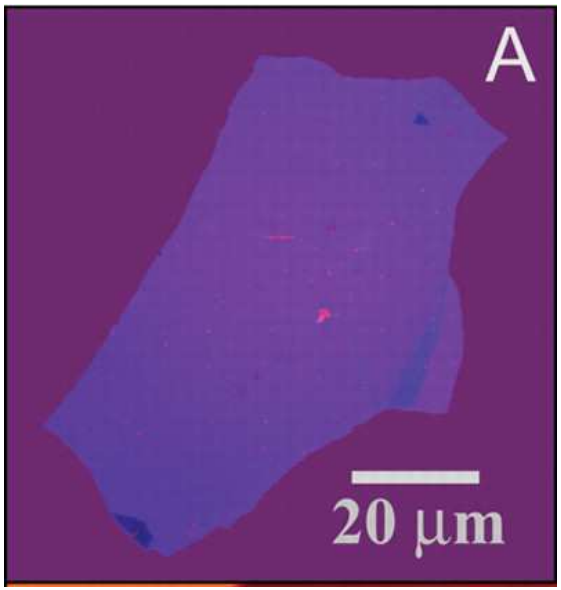

Photograph
in normal white light
of multilayer graphene flake
K. Novoselov *et al.*,Science **306**, 666 (2004)

Allotropes of carbon

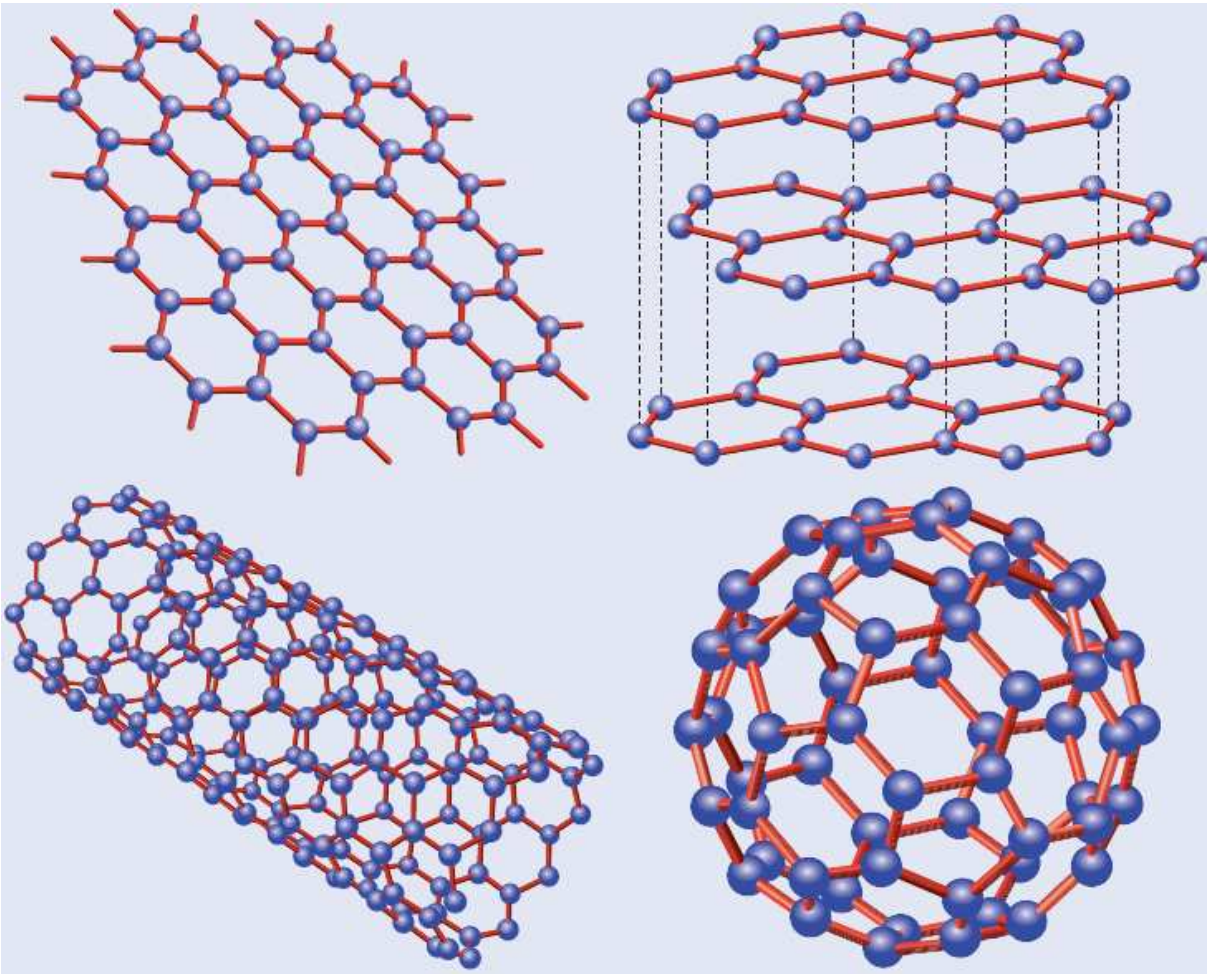

Well-known forms of carbon all are derived from graphene.

Field Effect Experiment

Field effect transistor

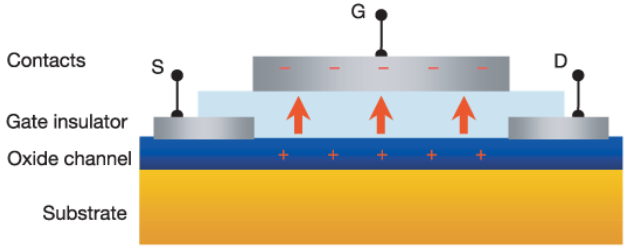

$V_g > 0$ means that we increase the number of electrons with increasing V_g, while we control holes for $V_g < 0$. Close to zero V_g, this film is a compensated semimetal.

Longitudinal conductivity as a function of gate voltage.

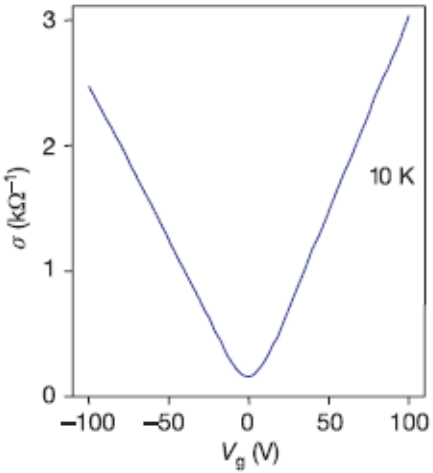

Novoselov *et al.*, Nature **308**, 197 (2005).

$\sigma_{min} = \frac{4e^2}{\pi h}$ – minimal conductivity

Orbitals of graphene

Carbon has 6 electrons, 2 are core electrons

4 are valence electrons: – one $2s$ and three $2p$ orbitals

single $2s$ and two $2p$ orbitals hybridize forming three "σ bonds" in the x-y plane

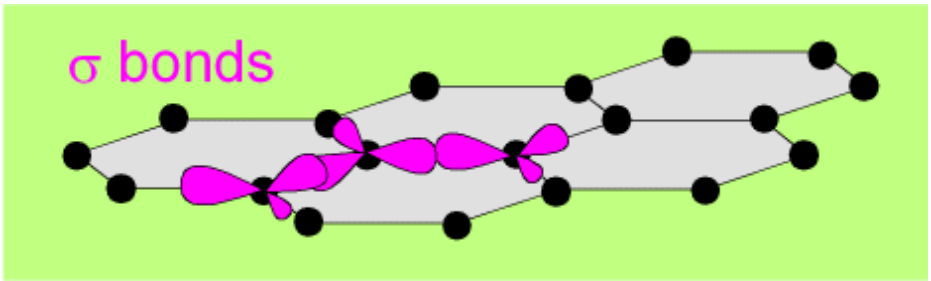

remaining $2p_z$ orbital ("π" orbital) is perpendicular to the $x-y$ plane

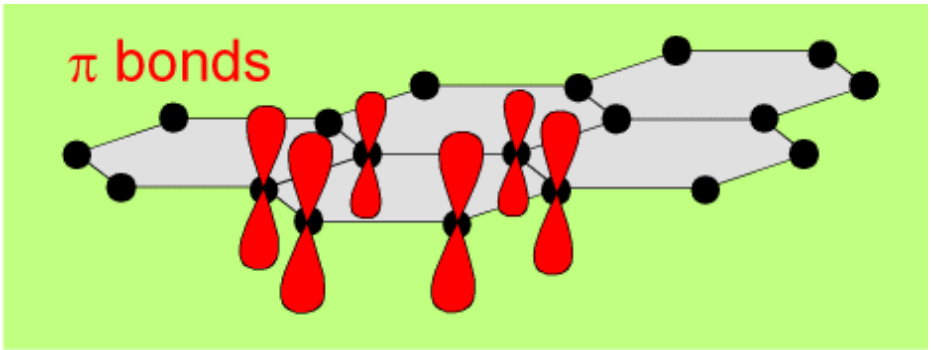

Lattice of graphene

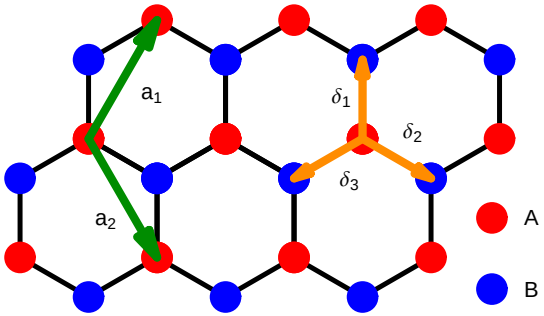

Graphene hexagonal lattice can be described in terms of two triangular sublattices, A and B.

$$H = t\sum_{\mathbf{n},i,\sigma} a^{\dagger}_{\mathbf{n},\sigma} b_{\mathbf{n}+\delta_i,\sigma} + h.c.,$$

$t \approx 3eV$, $a = \sqrt{3}a_{CC} = 2.46\text{Å}$ is the lattice constant, $i = 1,2,3$, $\sigma = \pm 1$ is the spin,

$$\delta_1 = a(0,\sqrt{3}/3),\ \delta_2 = a(\tfrac{1}{2},-\tfrac{\sqrt{3}}{6}),\ \delta_3 = a(-\tfrac{1}{2},-\tfrac{\sqrt{3}}{6}).$$

$$H = t\sum_{\mathbf{k},\sigma} \begin{pmatrix} a^{\dagger}_{\mathbf{k},\sigma} & b^{\dagger}_{\mathbf{k},\sigma} \end{pmatrix} \begin{pmatrix} 0 & f(\mathbf{k}) \\ f^*(\mathbf{k}) & 0 \end{pmatrix} \begin{pmatrix} a_{\mathbf{k},\sigma} \\ b_{\mathbf{k},\sigma} \end{pmatrix},\ f(\mathbf{k}) = \sum_i e^{i\mathbf{k}\delta_i}.$$

The π bands structure of a single graphene sheet is

$$E(\mathbf{k}) = \pm t|f(\mathbf{k})| = \pm t\sqrt{1 + 4\cos\frac{\sqrt{3}k_x a}{2}\cos\frac{k_y a}{2} + 4\cos^2\frac{k_y a}{2}}.$$

Band structure of graphene

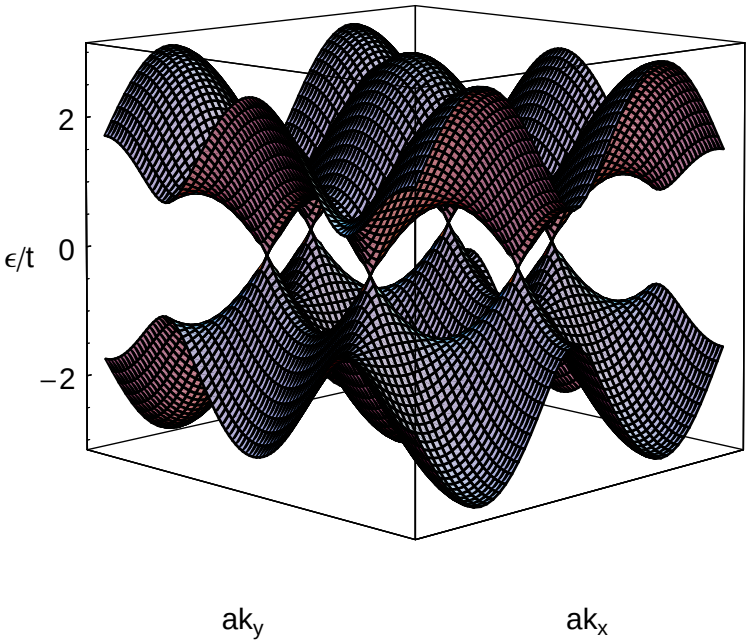

Two bands touch each other and cross the Fermi level in six $\mathbf{K}$ points located at the corners of the hexagonal 2D Brillouin zone.

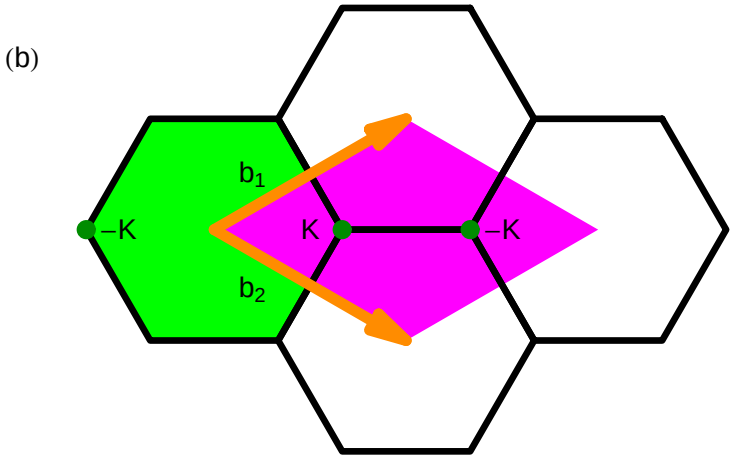

Hexagonal and rhombic extended Brillouin zone (BZ). Two non-equivalent $\mathbf{K}$ points in the extended BZ, $\mathbf{K}_- = -\mathbf{K}_+$.

P.R. Wallace, PR 71, 622 (1947).

Low-energy excitations in graphene

The low-energy excitations at two inequivalent $K, K' = (0, \pm 4\pi/3a)$ points have a linear dispersion $E_k = \pm \hbar v_F |\vec{k}|$ with $v_F = (\sqrt{3}/2\hbar) ta \approx 10^6$ m/s.
v_F plays role of the velocity of light $c \Rightarrow v_F = c/300$.
Each K point is described by its own spinor:

$$\psi_{K,\sigma} = \begin{pmatrix} \psi_{KA\sigma} \\ \psi_{KB\sigma} \end{pmatrix}$$

K, K' points are also called Dirac points. The Hamiltonian for K point

$$H_K = \hbar v_F \sum_{\sigma=\pm 1} \int \frac{d^2k}{(2\pi)^2} \psi^\dagger_{K\sigma} \begin{pmatrix} 0 & k_x - ik_y \\ k_x + ik_y & 0 \end{pmatrix} \psi_{K\sigma},$$

where the momentum $\mathbf{k} = (k_x, k_y)$ is given in a local coordinate system associated with a chosen K point.

Hamiltonian and Dirac equation for K point

The first quantized Hamiltonian (τ_i - the Pauli matrices)

$$\hat{H}_K = \hbar v_F \boldsymbol{\tau} \hat{\mathbf{k}} \Rightarrow -i\hbar v_F \boldsymbol{\tau} \boldsymbol{\nabla}.$$

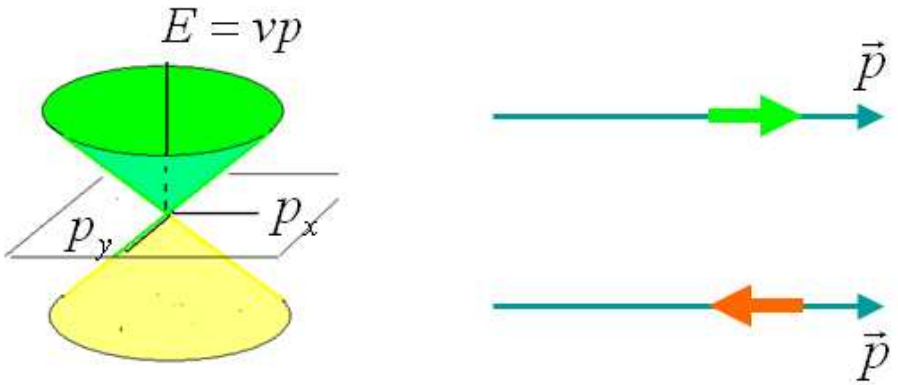

Pseudospin direction is linked to an axis determined by electronic momentum: for conduction and valence band electrons $\frac{\vec{\tau}\vec{p}}{|\vec{p}|} = \pm 1$.

Solutions of the Dirac equation $\hat{H}_K|\mathbf{k}\rangle = E|\mathbf{k}\rangle$:

$$|E_+, \mathbf{k}\rangle = \frac{e^{i\mathbf{kr}}}{\sqrt{2}} \begin{pmatrix} 1 \\ \frac{k_x + ik_y}{|\mathbf{k}|} \end{pmatrix}, |E_-, \mathbf{k}\rangle = \frac{e^{i\mathbf{kr}}}{\sqrt{2}} \begin{pmatrix} \frac{-k_x + ik_y}{|\mathbf{k}|} \\ 1 \end{pmatrix}, E_\pm = \pm \hbar v_F |\mathbf{k}|.$$

Scattering process $\mathbf{k} \to \mathbf{k}'$ due to a potential $V(\mathbf{r})$

$$|\langle \mathbf{k}'|V(\mathbf{r})|\mathbf{k}\rangle|^2 = |V(\mathbf{k}' - \mathbf{k})|^2 \cos^2(\theta_{k',k}/2).$$

Back scattering ($\mathbf{k} \to -\mathbf{k}'$, $\theta_{k',k} = \pi$) is suppressed!

Dirac equation for K point

The density of states of gapless graphene

$$\rho(E) = \sum_i d_i \int d^2k \delta(E - E_i(\mathbf{k})) = \frac{2|E|}{\pi\hbar^2 v_F^2},$$

where i numbers the energy bands and d their degeneracy ($d_i = 2 \times 2$ - spin and Dirac points). $\rho(E) \to 0$ when $E \to 0$.

Gapless graphene is semimetal!

Spinors at K, K' points can be also combined in one four-component Dirac spinor

$$\Psi_\sigma^T = (\psi_{KA\sigma}, \psi_{KB\sigma}, \psi_{K'B\sigma}, \psi_{K'A\sigma}),$$

and 4×4 γ-matrices $\gamma^\nu = \tilde{\tau}_3 \otimes (\tau_3, i\tau_2, -i\tau_1)$ belonging to a reducible representation of Dirac algebra.

We then have the standard form of the Dirac equation

$$\left(\gamma^0 \partial_t - v_F \boldsymbol{\gamma} \boldsymbol{\nabla}\right) \Psi = 0.$$

G. Semenoff, PRL **53**, 2449 (1984); D. DiVincenzo and E. Mele, PRB **29**, 1685 (1984).

Introducing a gap

$$H_K = \sum_{\sigma=\pm 1} \int \frac{d^2k}{(2\pi)^2} \psi^\dagger_{K\sigma} \begin{pmatrix} \Delta & \hbar v_F(k_x - ik_y) \\ \hbar v_F(k_x + ik_y) & -\Delta \end{pmatrix} \psi_{K\sigma}.$$

The presence of a gap $\Delta \neq 0$ changes the spectrum:
$E(\mathbf{k}) = \pm\sqrt{\hbar^2 v_F^2 \mathbf{k}^2 + \Delta^2}$.
A gap can be induced by interaction with substrate.

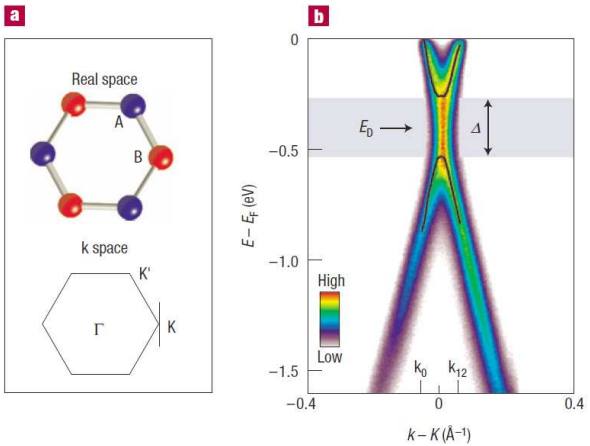

S.Y. Zhou *et al.*, Nature Mat. **6**, 770 (07).

Observation of the gap opening in single-layer epitaxial graphene on a SiC substrate at the K point.
(a) Structure of graphene in the real and momentum space.
(b) ARPES intensity map taken along the black line in the inset of (a).

Berry phase, Berry curvature and Chern-Pontryagin numbers

Dirac fermions of pseudospin 1/2 in two or three dimensions are described by the Hamiltonian

$$H(\mathbf{k}) = \sum_{i=1}^{3} d_i(\mathbf{k})\tau_i,$$

and $d_i(\mathbf{k})$ are the functions of two- or three dimensional wave number $\mathbf{k}$. The energies are $\epsilon(\mathbf{k})_\pm = \pm|\mathbf{d}|$ and eigenstates are

$$\psi_+(\mathbf{k}) = C\begin{pmatrix} d_3 + d \\ d_1 + id_2 \end{pmatrix}, \psi_-(\mathbf{k}) = C\begin{pmatrix} -d_1 + id_2 \\ d_3 + d \end{pmatrix}, C = \frac{1}{\sqrt{2d(d+d_3)}}.$$

Berry connection:

$$\mathcal{A}_i^\pm(\mathbf{k}) = i\langle\psi_\pm(\mathbf{k})|\nabla_{k_i}\psi_\pm(\mathbf{k})\rangle = \mp\frac{d_1\partial_i d_2 - d_2\partial_i d_1}{2d(d+d_3)}.$$

Berry curvature

$$\Omega_i = (\boldsymbol{\nabla}_k \times \mathcal{A})_i = \epsilon_{ijk}\partial_j\mathcal{A}_k = \frac{1}{2}\epsilon_{ijk}\mathcal{F}_{jk}.$$

Berry phase, Berry curvature and Chern-Pontryagin numbers

$$\mathcal{F}_{ij}^{\pm}(\mathbf{k}) = \mp \frac{1}{2d^3} \epsilon_{\alpha\beta\gamma} d_\alpha(\mathbf{k}) \frac{\partial d_\beta(\mathbf{k})}{\partial k_i} \frac{\partial d_\gamma(\mathbf{k})}{\partial k_j}.$$

Berry phase along a closed contour around the K point :

$$\Phi(\Gamma) = \oint_\Gamma d\mathbf{k} \mathcal{A}(\mathbf{k}).$$

The topological invariant in two dimensions (the first Chern-Pontryagin number) is determined by the winding number of the vector $\mathbf{d}(\mathbf{k})$ around the origin

$$\nu = \frac{1}{4\pi} \int d^2k \epsilon_{ij} \mathcal{F}_{ij}(\mathbf{k}) = \lim_{|\mathbf{k}|\to\infty} \frac{1}{2\pi} \oint_\Gamma d\mathbf{k} \mathcal{A}(\mathbf{k}).$$

Nice review papers: Xiao et al., Berry phase effects on electronic properties, Rev. Mod. Phys. **82**, 1959 (2010); Hasan&Kane, Topological insulators, Rev. Mod. Phys. **82**, 3045 (2010).

For gapped graphene $d_1 = k_x, d_2 = k_y, d_3 = \Delta$, hence

$$\mathcal{A}_i^{\pm} = \mp\epsilon_{ij}\frac{k_j}{2\mathbf{k}^2}\left(1 - \frac{\Delta}{\sqrt{\mathbf{k}^2 + \Delta^2}}\right),$$

$$\mathcal{F}_{ij}^{\pm}(\mathbf{k}) = \mp\epsilon_{ij}\frac{\Delta}{2(\mathbf{k}^2 + \Delta^2)^{3/2}}.$$

Berry phases and Chern-Pontryagin numbers:

$$\Phi^{\pm} = \mp\pi\left(1 - \frac{\Delta}{\sqrt{\mathbf{k}^2 + \Delta^2}}\right),$$

$$\nu^{\pm} = \mp\frac{1}{2}.$$

QED form of Lagrangian

$$L = \int d^2\mathbf{r}\,\bar{\Psi}_\sigma(t,\mathbf{r})\left[\gamma^0(i\hbar\partial_t+\mu)+v_F\hbar\left(\gamma^1 i\partial_x+\gamma^2 i\partial_y\right)-\ \Delta\right]\Psi_\sigma(t,\mathbf{r})$$
$$-\frac{e^2}{2\kappa}\int d^2\mathbf{r}\,d^2\mathbf{r}'\,\bar{\Psi}_\sigma(t,\mathbf{r})\gamma^0\Psi_\sigma(t,\mathbf{r})\frac{1}{|\mathbf{r}-\mathbf{r}'|}\bar{\Psi}_\sigma(t,\mathbf{r}')\gamma^0\Psi_\sigma(t,\mathbf{r}'),$$

$\bar{\Psi}=\Psi^\dagger\gamma^0$. μ is the chemical potential which can be controlled by the gate voltage V_g: $\mu\propto \mathrm{sgn}(V_g)\sqrt{|V_g|}\in[-3600\mathrm{K},3600\mathrm{K}]$ when $V_g\in[-100\mathrm{V},100\mathrm{V}]$; $\mu>0$ – electrons.

QED form of Lagrangian

$$L = \int d^2\mathbf{r}\,\bar{\Psi}_\sigma(t,\mathbf{r})\left[\gamma^0(i\hbar\partial_t+\mu)+v_F\hbar\left(\gamma^1 i\partial_x+\gamma^2 i\partial_y\right)-\Delta\right]\Psi_\sigma(t,\mathbf{r})$$
$$-\frac{e^2}{2\kappa}\int d^2\mathbf{r}\,d^2\mathbf{r}'\,\bar{\Psi}_\sigma(t,\mathbf{r})\gamma^0\Psi_\sigma(t,\mathbf{r})\frac{1}{|\mathbf{r}-\mathbf{r}'|}\bar{\Psi}_\sigma(t,\mathbf{r}')\gamma^0\Psi_\sigma(t,\mathbf{r}'),$$

$\bar{\Psi}=\Psi^\dagger\gamma^0$. μ is the chemical potential which can be controlled by the gate voltage V_g: $\mu\propto \mathrm{sgn}(V_g)\sqrt{|V_g|}\in[-3600\mathrm{K},3600\mathrm{K}]$ when $V_g\in[-100\mathrm{V},100\mathrm{V}]$; $\mu>0$ – electrons.

Δ is a possible excitonic gap (Dirac mass) generated due to Coulomb interaction. Magnetic field favors gap opening: Magnetic catalysis phenomenon

Symmetry

- The Lagrangian L possesses "flavor" $U(4)$ symmetry
- 16 generators read (spin $\otimes$ valley)

$$\frac{\sigma^\alpha}{2} \otimes I_4,\ \frac{\sigma^\alpha}{2i} \otimes \gamma^3,\ \frac{\sigma^\alpha}{2} \otimes \gamma^5, \text{ and } \frac{\sigma^\alpha}{2} \otimes \gamma^3\gamma^5,$$

$\gamma^3 = i\tilde{\tau}_1 \otimes \tau_0,\ \gamma^5 = -i\tilde{\tau}_2 \otimes \tau_0,\ \gamma^3\gamma^5 = \tilde{\tau}_3 \otimes \tau_0,$
$\sigma^\alpha = (\sigma_0, \boldsymbol{\sigma})$.

- The inclusion of the Zeeman interaction term $\mu_B B\bar{\Psi}\gamma^0\sigma_3\Psi$ breaks $U(4)$ down to $U(2)_+ \otimes U(2)_-$ ($\mu_B = e\hbar/(2mc)$ - the Bohr magneton).
- Dirac mass $\Delta\bar{\Psi}\Psi$ further breaks $U(2)_s$ down to $U(1)_s$.

QED form of Lagrangian

In graphene the quasiparticles are localized on two-dimensional plane while a gauge field responsible for interaction propagates in a three-dimensional bulk (braneworld model).

$$
\begin{aligned}
S &= \int d^3 r dt \left[-\frac{1}{4} F_{\mu\nu}^2 - A_0 j_0 + \frac{1}{c} \vec{A}\vec{j} \right. \\
&+ \left. \bar{\Psi}_\sigma(r,t) \left(\gamma^0 (i\hbar\partial_t + \mu) + i\hbar v_F \gamma^i \partial_i - \Delta \right) \Psi_\sigma(r,t) \delta(z) \right], \\
j_0 &= e \bar{\Psi}_\sigma(r,t) \gamma^0 \Psi_\sigma(r,t) \delta(z), \\
j_i &= e v_F \bar{\Psi}_\sigma(r,t) \gamma_i \Psi_\sigma(r,t) \delta(z).
\end{aligned}
$$

Integration over z-coordinate gives a nonlocal interaction for quasiparticles in a plane:

$$
\begin{aligned}
S &= \int d^2 r dt \left[-\frac{1}{4} F_{ab} \frac{1}{\sqrt{-\partial^2}} F_{ab} + \bar{\Psi}_\sigma(r,t) \left(\gamma^0 (i\hbar\partial_t - eA_0 + \mu) \right. \right. \\
&- \left. \left. v_F \vec{\gamma} (i\hbar\vec{\partial} - e\vec{A}/c) - \Delta \right) \Psi_\sigma(r,t) \right].
\end{aligned}
$$

Landau levels

Landau, 1930; Bronstein and Frenkel, 1930 - Schrodinger equation:

$$E(n,k_z)=\frac{p_z^2}{2m}+\hbar\omega_c\left(n+\frac{1}{2}\right)$$

In nonrelativistic case the distance between LL coincides with the cyclotron energy, $\hbar\omega_c=\frac{e\hbar B}{m_e c}\sim 1.35K\cdot B[\text{Tesla}]$.
For Dirac equation (Rabi, 1928):

$$E(n,k_z)=\pm\sqrt{\hbar c|eB|\left(n+\frac{1}{2}\pm\frac{1}{2}\right)+c^2p_z^2+m^2c^4}$$

For two-dimensional relativistic-like system (gapless graphene),

$$E_n=\pm\sqrt{2n\hbar v_F^2|eB|/c},\ n=0,1,\ldots.$$

the energy scale, characterizing the distance between Landau levels, is $\hbar\omega_L=v_F\sqrt{\frac{\hbar 2eB}{c}}\sim 424K\cdot\sqrt{B[\text{Tesla}]}$ for $v_F\approx 10^6\text{m/s}$!
QHE effect is observed in graphene at room temperature!

Dirac equation in a magnetic field

The Dirac equation has a block diagonalized form

$$\begin{pmatrix} E-\Delta & -\hbar v_F(D_x - iD_y) \\ \hbar v_F(D_x + iD_y) & E+\Delta \end{pmatrix} \begin{pmatrix} \psi_{KA} \\ \psi_{KB} \end{pmatrix} = 0,$$

$$\begin{pmatrix} E+\Delta & -\hbar v_F(D_x - iD_y) \\ \hbar v_F(D_x + iD_y) & E-\Delta \end{pmatrix} \begin{pmatrix} \psi_{K'B} \\ \psi_{K'A} \end{pmatrix} = 0.$$

Covariant derivative $D_i = \partial_i + (ie/\hbar c)A_i$, $A_i = (-By, 0)$ - Landau gauge for the vector potential.

Spectrum

$$E_n = \pm M_n = \pm\sqrt{\Delta^2 + 2n|eB|\hbar v_F^2/c}, \quad n = 0, 1, 2, \ldots,$$

but the degeneracy of the levels $n = 0$ and $n \geq 1$ is different!

Solution for the upper block – K point

$$\psi_{nk}^{(+)} = \frac{\exp(ikx)}{\sqrt{2\pi l}} \frac{1}{\sqrt{2M_n}} \begin{bmatrix} \sqrt{M_n + \Delta}\, w_{n-1}(\xi) \\ i\sqrt{M_n - \Delta}\, w_n(\xi) \end{bmatrix}, \quad n \geq 1,$$

$$\psi_{0k}^{(-)} = \frac{\exp(ikx)}{\sqrt{2\pi l}} \begin{bmatrix} 0 \\ w_0(\xi) \end{bmatrix}, \quad n = 0, \quad E_0 = -\Delta$$

$$\psi_{nk}^{(-)} = \frac{\exp(ikx)}{\sqrt{2\pi l}} \frac{1}{\sqrt{2M_n}} \begin{bmatrix} \sqrt{M_n - \Delta}\, w_{n-1}(\xi) \\ -i\sqrt{M_n + \Delta}\, w_n(\xi) \end{bmatrix}, \quad n \geq 1$$

$l = \sqrt{\hbar c/|eB|}$ is the magnetic length. Asymmetry in the spectrum!

$$w_n(\xi) = \left(\pi^{1/2} 2^n n!\right)^{-1/2} e^{-\xi^2/2} H_n(\xi), \quad \xi = y/l - kl.$$

$H_n(\xi)$ are the Hermite polynomials.

Solution for the lower block - K' point

$$\psi_{0k}^{(+)} = \frac{\exp(ikx)}{\sqrt{2\pi l}} \begin{bmatrix} 0 \\ w_0(\xi) \end{bmatrix}, \quad n = 0, \quad E_0 = \Delta$$

$$\psi_{nk}^{(+)} = \frac{\exp(ikx)}{\sqrt{2\pi l}} \frac{1}{\sqrt{2M_n}} \begin{bmatrix} -i\sqrt{M_n - \Delta}\, w_{n-1}(\xi) \\ \sqrt{M_n + \Delta}\, w_n(\xi) \end{bmatrix}, \quad n \geq 1,$$

$$\psi_{nk}^{(-)} = \frac{\exp(ikx)}{\sqrt{2\pi l}} \frac{1}{\sqrt{2M_n}} \begin{bmatrix} i\sqrt{M_n + \Delta}\, w_{n-1}(\xi) \\ \sqrt{M_n - \Delta}\, w_n(\xi) \end{bmatrix}, \quad n \geq 1$$

The spinors $\psi^{(+)}$ and $\psi^{(-)}$ describe solutions with positive and negative energy, respectively. The energies do not depend of k - flat bands! The $n = 0$ Landau level is special: $E_n = \pm\sqrt{\Delta^2 + 2nv_F^2\hbar|eB|}/c \Rightarrow E_0 = \pm\Delta$ – it does not depend of a magnetic field and its degeneracy is half of the degeneracy of LL with $n \geq 1$.

Dirac Landau levels

$B = 0$ and zero gap, $\Delta = 0$

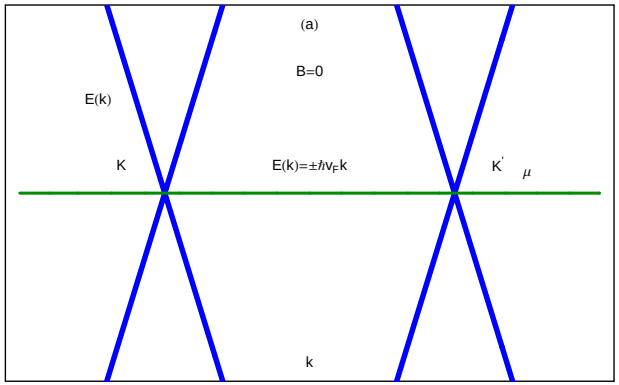

(a) The low-energy linear-dispersion. $\mu = 0$ is a neutral point.

$B = 0$ and finite gap, $\Delta \neq 0$

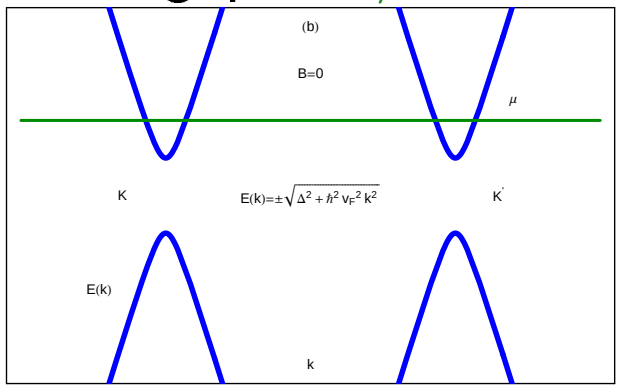

(b) A possible modification of the spectrum by the finite gap Δ. μ is shifted from zero by the gate voltage.

$B \neq 0$ and finite gap, $\Delta \neq 0$

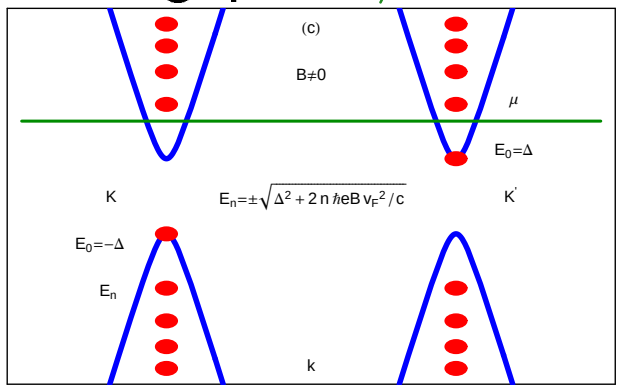

(c) Landau levels E_n. Notice that for K point $E_0 = -\Delta$ and for K' point $E_0 = \Delta$. Then the degeneracy of $n = 0$ level is half of the degeneracy of LL with $n \neq 0$.

Oscillations of density of states

DOS is the sum over LL ($E_n = \sqrt{2n|eB|\hbar v_F^2}/c$:

$$\rho(E) = -\frac{1}{\pi}\mathrm{Im}\,\mathrm{tr}\frac{1}{E + i0 - H} = \frac{2eB}{\pi\hbar c}\times$$

$$\left[\delta(E) + \sum_{n=1}^{\infty}(\delta(E - E_n) + \delta(E + E_n))\right] \Rightarrow \rho(E) = \frac{2|E|}{\pi\hbar^2 v_F^2},$$

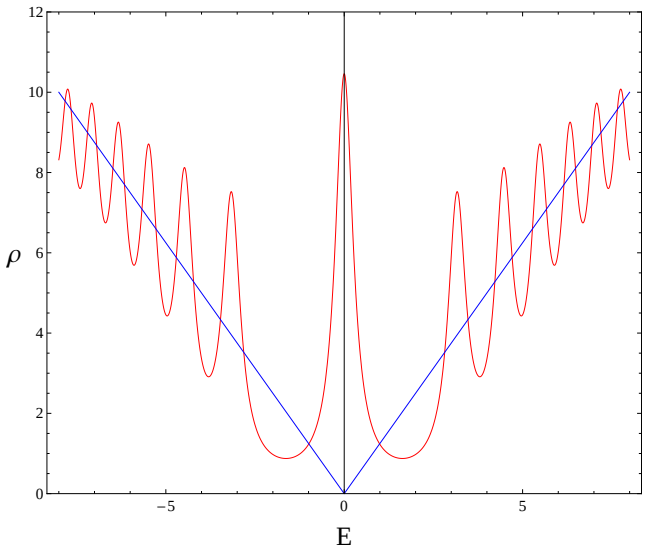

In presence of scattering on impurities the levels are broadened ($\delta(E) \to \Gamma/\pi(E^2 + \Gamma^2)$, the DOS is oscillating. Note that $\rho(E = 0) \neq 0$!

Manifestation of Berry's Phase

Oscillating part of conductivity (Shubnikov de Haas effect)

$$\sigma_{xx} \propto \sum_{k=1}^{\infty} \cos\left[2\pi k\left(\frac{B_f}{B}+\frac{1}{2}+\beta\right)\right] R_T(k) R_D(k),\ B_f = \frac{\hbar c n}{e d},$$

where d is the LL degeneracy and β is Berry's phase. For $\beta = 0$ we get classical Lifshits-Kosevich formula in the case of the parabolic spectrum $E(\mathbf{p}) = \mathbf{p}^2/2m$.

$$\left.\begin{array}{l} E_n = \frac{e\hbar B}{m_e c}\left(n+\frac{1}{2}\right); \\ \beta = 0. \end{array}\right\} \Leftarrow$$

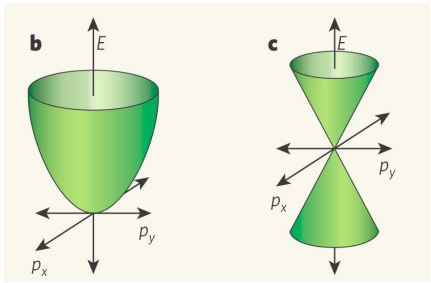

$$\text{Dirac} \Rightarrow \left\{\begin{array}{l} E_n = v_F\sqrt{\frac{\hbar 2neB}{c}}; \\ \beta = -1/2. \end{array}\right.$$

Dingle and temperature amplitude factors:

$$R_D(k,\mu) = \exp\left(-2\pi k\frac{c|\mu|\Gamma}{v_F^2 e\hbar B}\right), \qquad R_T(k,\mu) = \frac{2\pi^2 kTc|\mu|/(v_F^2 e\hbar B)}{\sinh\frac{2\pi^2 kTc|\mu|}{v_F^2\hbar eB}}$$

depend on chemical potential μ ($n = \frac{\mu^2}{\pi v_F^2\hbar^2}\mathrm{sgn}\mu$)- there is a dependence on carrier concentration n!

Oscillating conductivity - experiment

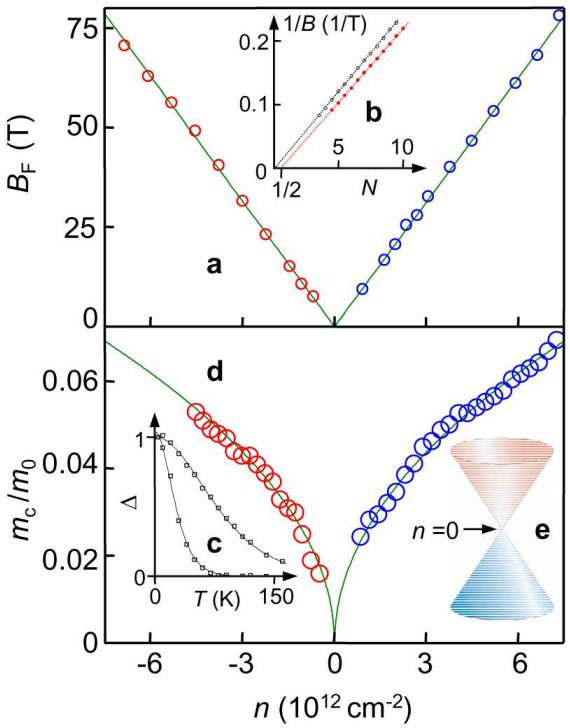

K.S. Novoselov, *et al.*, Nature 438, 197 (2005)

a) Dependence of B_F on carrier concentration n
b) Landau fan diagrams used to find B_F. N is the number associated with different minima of oscillations. The curves extrapolate to different origins: to $N = 1/2$ (in one layer) and 0 (two and more layers).
c) The behavior of SdHO amplitude as a function of T for two different carrier concentrations.
d) Cyclotron mass m_c ($\sim$ Fermi energy $|\mu|$ for Dirac quasiparticles!) of electrons and holes as a function of their concentration.
$m_c = |\mu|/v_F^2 = \sqrt{\pi\hbar^2|n|}/v_F^2$ The effective carrier mass $= 0$, because $E(\mathbf{k}) = \pm\hbar v_F|\mathbf{k}|$.

Quantum Hall Effect

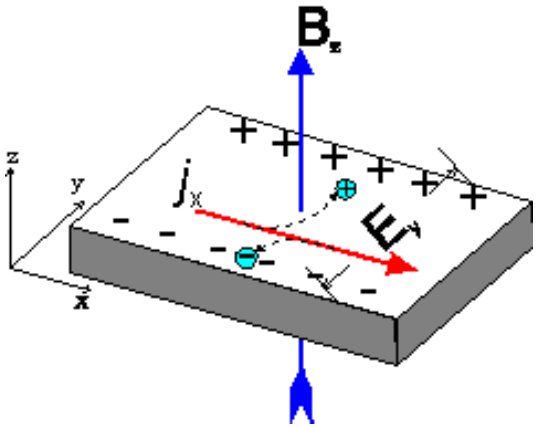

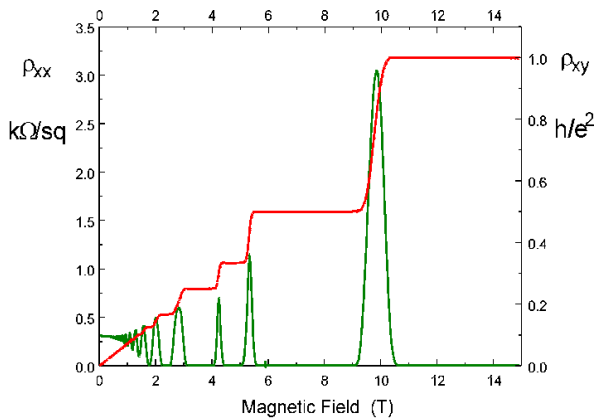

Classical Hall effect (Edwin Hall, 1879) is the production of a voltage difference (the Hall voltage) across an electrical conductor, transverse to an electric current in the conductor and to an applied magnetic field perpendicular to the current: $j_x = \sigma_{xy} E_y$, $\sigma_{xy} = -\frac{nec}{B}$.

$$\rho_{xx} = \frac{\sigma_{xx}}{\sigma_{xx}^2 + \sigma_{xy}^2}, \; \rho_{xy} = -\frac{\sigma_{xy}}{\sigma_{xx}^2 + \sigma_{xy}^2}.$$

Quantum Hall effect (Klaus von Klitzing, 1980):

$$1. \sigma_{xx} = 0,$$

$$2. \sigma_{xy} = -\frac{nec}{B} \Rightarrow -\frac{e^2}{h}\nu, \; \nu = \left[\frac{nch}{eB}\right] = 0, 1, \ldots.$$

Hall conductivity in graphene

The Hall (transverse) conductivity) calculated by means of the Kubo formula (Gusynin et al., PRL, 2005):

$$\sigma_{xy} = \frac{e^2}{h}\mathrm{sgn}(eB)\left[\tanh\frac{\mu+\Delta}{2T} + \tanh\frac{\mu-\Delta}{2T} + 2\sum_{n=1}^{\infty}\left(\tanh\frac{\mu+\sqrt{\Delta^2+2|eB|n}}{2T} + \tanh\frac{\mu-\sqrt{\Delta^2+2|eB|n}}{2T}\right)\right]$$

When $\Delta = 0$ and $T \to 0$ we obtain

$$\sigma_{xy} = \frac{2e^2}{h}\mathrm{sgn}(eB)\mathrm{sgn}\mu\left[1 + 2\sum_{n=1}^{\infty}\theta\left(|\mu| - \sqrt{2|eB|n}\right)\right]$$

$$= \frac{2e^2}{h}\mathrm{sgn}(eB)\mathrm{sgn}\mu\left(1 + 2\left[\frac{\mu^2 c}{2\hbar|eB|v_F^2}\right]\right).$$

$[x]$ denotes the integer part of x.

Hall effect in graphene

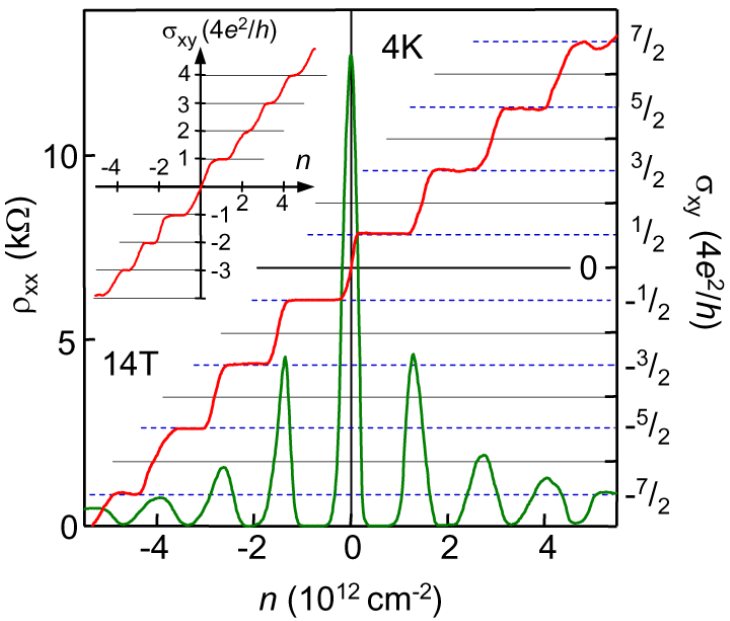

Experiment: Novoselov, Geim *et al.*, Nature **438**, 197 (2005). Kim, Stormer, *et al.*, Nature **438**, 201 (2005). Hall conductivity σ_{xy} and longitudinal resistivity ρ_{xx} of graphene as a function of their concentration at B =14T.

Theory:Hall conductivity

$\sigma_{xy} = e^2\nu/h,$

$\nu = 4(n+1/2) = \pm 2, \pm 6, \pm 10, \ldots$

– filling factor, $n = 0, \pm 1, \pm 2, \cdots$.

Factor 4 describes the degeneracy of Landau levels: 4 = spin× valleys. Observation of IQHE is the ultimate proof of the existence of Dirac quasiparticles in graphene. Standard of resistance from graphene:

$R = h/e^2 = 25812.807957(18)\text{Om}.$

Hydrogen atom in the Dirac theory

$$E_{nj} = mc^2 \left[1 + \frac{(Z\alpha)^2}{\left(n - |\kappa| + \sqrt{\kappa^2 - (Z\alpha)^2} \right)^2} \right]^{-1/2}, \quad \kappa = \mp(j + 1/2)$$

$n = 1, 2, 3, \ldots \Rightarrow$ energy of the lowest discrete level $1S_{1/2}$,

$E_1 = mc^2 \sqrt{1 - (Z\alpha)^2}$

Dependence of energy levels with $j = 1/2$ on $\zeta = Z/137$.

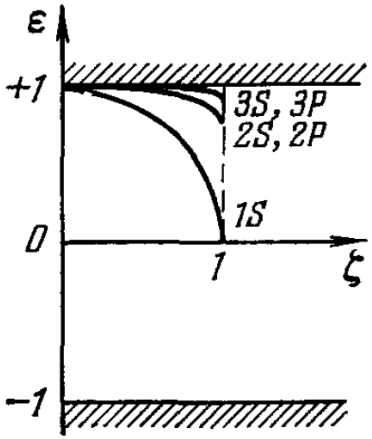

What happens for $Z > 137$?

Pomeranchuk and Smorodinsky (1945)

Taking into account finite size of nuclei.

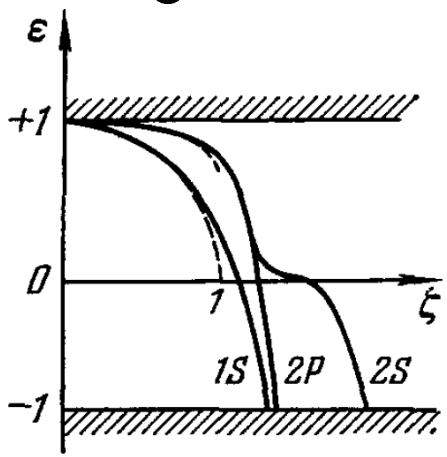

Discrete levels exist for $137 < Z < 170$.

Gapped graphene in the Coulomb potential

$$[-\hbar v_F\,(i\sigma_1\partial_x + i\sigma_2\partial_y) + \sigma_3\Delta + V(r)]\,\Psi(r) = E\Psi(r),$$

$$V(r) = -\frac{Ze^2}{\kappa r}\theta(r-R) - \frac{Ze^2}{\kappa R}\theta(R-r),$$

where κ is a dielectric constant of a substrate. The wave function

$$\Psi = \frac{1}{r}\begin{pmatrix} e^{i\phi(j-1/2)}\,a(r) \\ i\,e^{i\phi(j+1/2)}\,b(r) \end{pmatrix}, \quad j = \pm 1/2, \pm 3/2, \cdots,$$

[j is full angular momentum] and we obtain the system of equations

$$a' - (j+\frac{1}{2})\frac{a}{r} + \frac{E+\Delta-V(r)}{\hbar v_F}b = 0,\; b' + (j-\frac{1}{2})\frac{b}{r} - \frac{E-\Delta-V(r)}{\hbar v_F}a = 0.$$

The Dirac equation is solved in terms of the Whittaker functions $W_{\mu,\nu}(\rho)$.

Coulomb center: bound states

The spectrum for pure Coulomb potential $V(r) = -Ze^2/\kappa r$ (Balmer-like formula):

$$E_{nj} = \Delta \left[1 + \frac{Z^2\alpha^2}{(\sqrt{j^2 - (Z\alpha)^2} + n)^2} \right]^{-1/2}, \begin{cases} n = 0, 1, 2, 3, ..., \; j > 0, \\ n = 1, 2, 3, ..., \quad j < 0, \end{cases}$$

where $\alpha = e^2/\kappa\hbar v_F$ - "fine structure constant" in graphene, for $\kappa = 1$ we have $\alpha \approx 2.2$. The lowest energy level

$$E_{0,j=1/2} = \Delta\sqrt{1 - (2Z\alpha)^2}.$$

For $Z\alpha > 1/2$ the energy becomes imaginary, i.e., the fall into the center phenomenon occurs (similar to the Dirac equation in $3+1$ dimensions).

Supercritical Coulomb center: resonant states

For finite size R of the Coulomb center discrete levels exist for $Z\alpha > 1/2$:

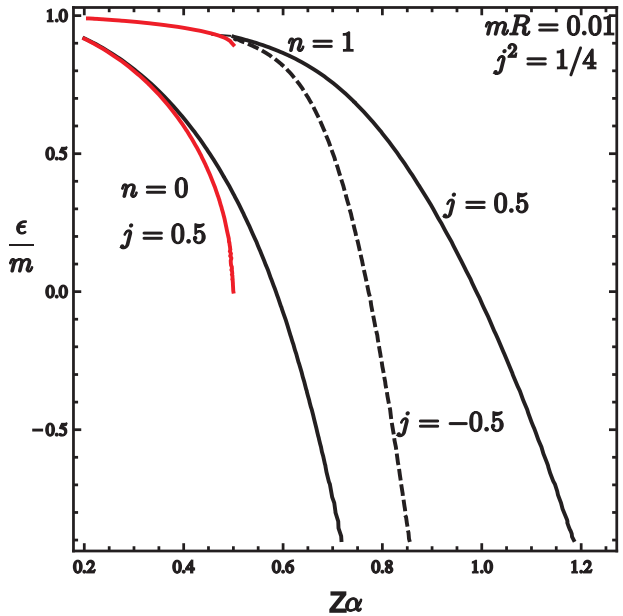

The energy levels in the regularized Coulomb potential.

Gamayun et al., PRB 80, 165429 (2009).

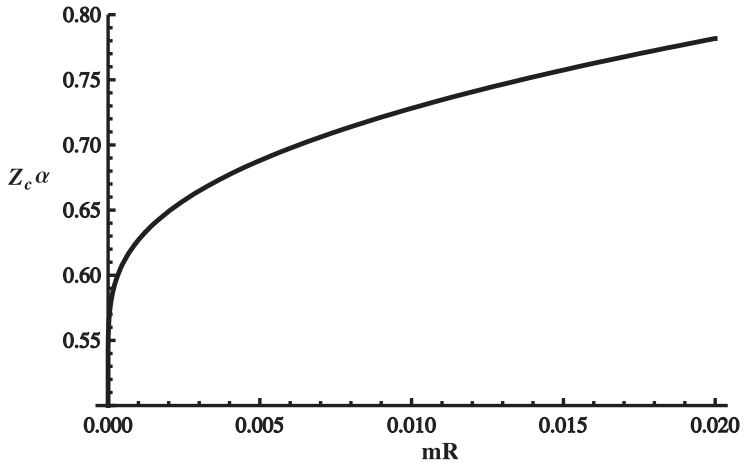

The lowest energy level $E_{0,1/2}$ dives into continuum for $Z\alpha > Z_c\alpha$:

$$Z_c\alpha \simeq \frac{1}{2} + \frac{\pi^2}{\log^2(cR\Delta)}, \quad R\Delta \ll 1$$

Gapless graphene

$Z\alpha < 1/2$ – no discrete or resonant states,

$Z\alpha > 1/2$ – we find quasidiscrete levels with imaginary energy:

$$E_n^{(0)} = -\,(0.18 + 0.17i)\, R^{-1} \exp\left[-\frac{\pi n}{\sqrt{Z^2\alpha^2 - 1/4}}\right],\ n = 1, 2, \ldots.$$

The resonant states with $E_n^{(0)}$ describe the spontaneous emission of positively charged holes when electron bound states dive into the lower continuum. The finite gap (mass) results in decreasing the width of resonance,

$$E_n = E_n^{(0)} - \Delta + \frac{\Delta^2}{|E_n^{(0)}|}\,(0.24 + 0.20i)\,,$$

and, therefore, increases stability of the system.

Artificial atoms on graphene

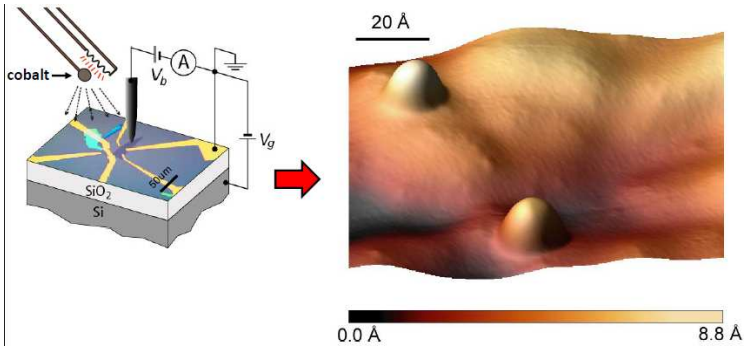

V.W. Brar, *et al.*, Nature Phys. 7, 43 (11).

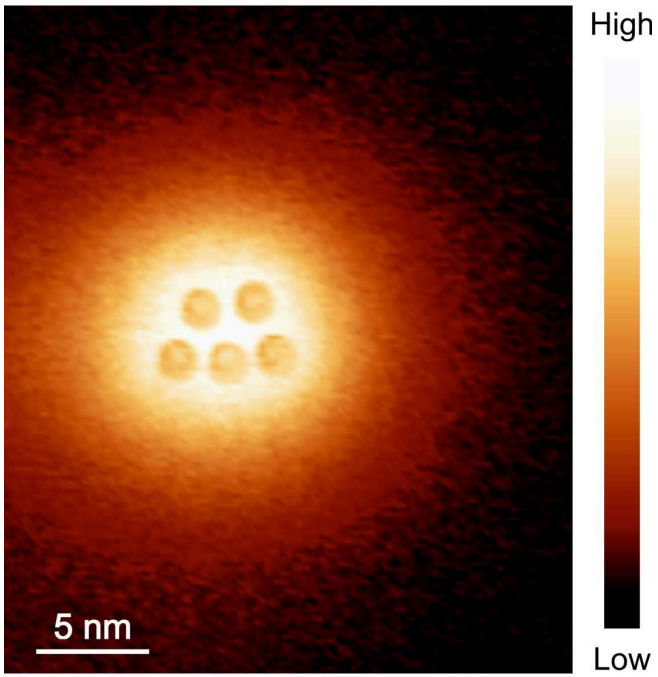

Y. Wang, *et al.*, Sciencexpress, 7 March 2013.

Spatial distribution of atomic collapse state around an artificial nucleus at the energy of the supercritical quasibound state resonance. Artificial atoms are made on gated graphene devices of Ca.

$dI/dV \sim \rho(E, r)$ map near a five–Ca dimer cluster.

$$\rho(E, r) = 4 \sum_{nj} \delta_\gamma(E - E_{nj}) |\psi_{nj}(r)|^2$$

$$\delta_\gamma(E) = \gamma/\pi(E^2 + \gamma^2).$$

Resonances in artificial nuclei on graphene: atomic collapse

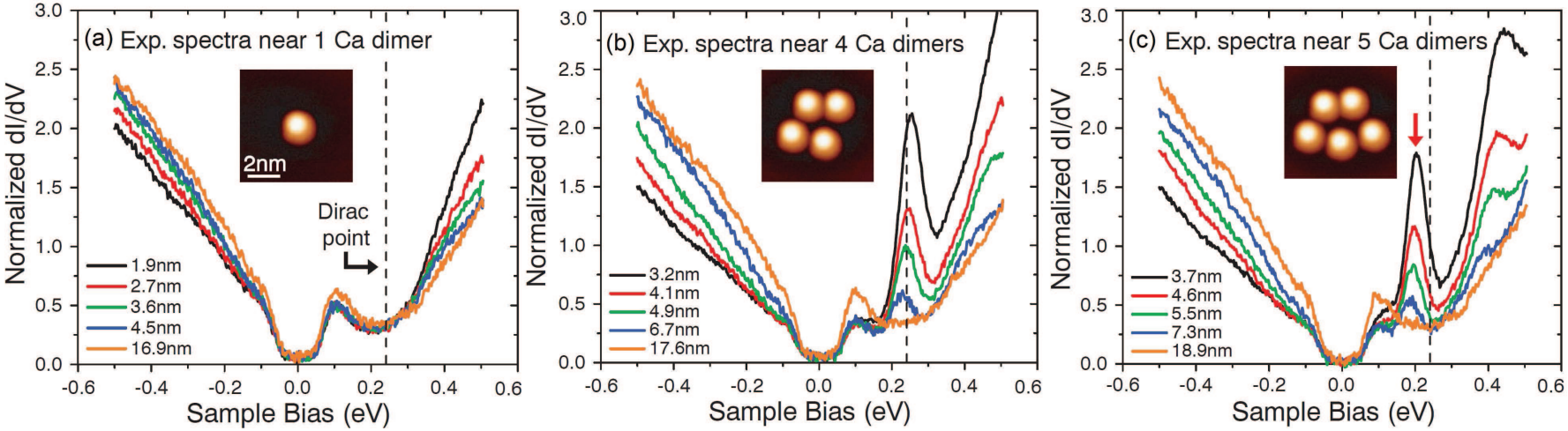

Spectra $dI/dV \sim \rho(E = eV, r)$ at different distances from the center of Ca dimer clusters (i.e., artificial nuclei) as functions of a simple bias V(meV). For free massless Dirac fermions $\rho(E) = \frac{2|E|}{\pi(\hbar v_F)^2}$

Experiment: Y. Wang, *et al.*, Science 340, 734 (2013).

Dirac equation with two equally charged impurities in gapped graphene

$$H = v_F \boldsymbol{\tau} \boldsymbol{p} + \Delta \tau_z + V(r), V(\mathbf{r}) = -\frac{Ze^2}{\kappa}\left(\frac{1}{r_1} + \frac{1}{r_2}\right),$$

$r_{1,2} = |\mathbf{r} \pm \mathbf{R}/2|$ measure distances from Coulomb impurities to the electron. Charges of impurities are subcritical, whereas their total charge exceeds a critical one. The critical distance $R_{\rm cr}$ in the system of two charged centers is defined as that at which the electron bound state with the lowest energy reaches the boundary of the lower continuum $E = -\Delta$ $(\zeta = 2Z\alpha/\kappa, \gamma = \sqrt{4\zeta^2 - 1})$.
Approximate analytical solution:

$$R_{\rm cr} = \frac{v_F^2}{\Delta\zeta} \exp\left[-\frac{2}{\gamma}\left(\cot^{-1}\frac{1 - 2\sqrt{1-\zeta^2}}{\gamma} - \arg\Gamma(1 + i\gamma)\right)\right].$$

The width of the quasistationary state close to the boundary of the lower continuum:

$$\Gamma \propto \exp\left[-2\pi\left(\tilde{\beta}\sqrt{\frac{R}{R_{\rm cr}-R}}-\sqrt{\zeta^2-1/4}\right)\right],$$

$$\tilde{\beta}=\sqrt{\frac{8\zeta^2+7}{24}},\ R\lesssim R_{\rm cr},$$

which tends to zero when $R \to R_{\rm cr}$.

Sobol et al., Phys. Rev. B88, 205116 (2013).

Charged impurity in a magnetic field

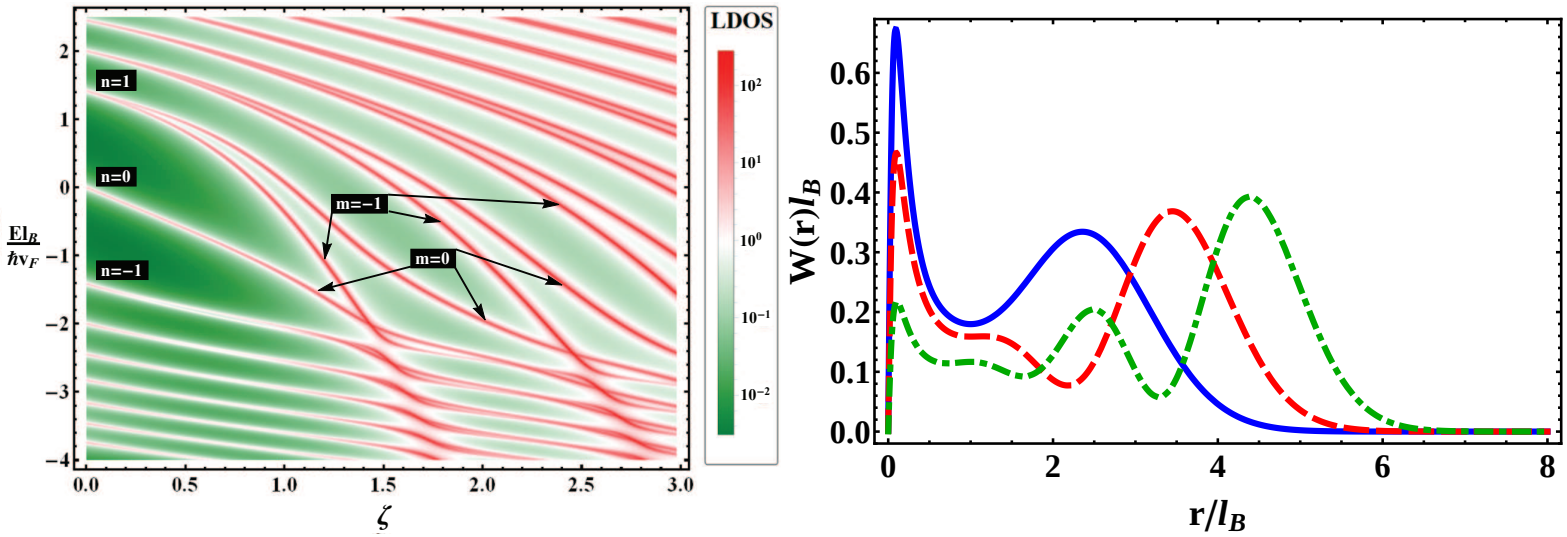

Left: Local density of states at the impurity position ($r = 0$) as a function of coupling ζ and energy E in the magnetic field $B = 10$ T. Black labels indicate the Landau level numbers n and orbital quantum numbers m. Anticrossing for levels $n = 0, m = 0$ and $n = -1, m = 0$.

Right: The radial functions of the electron density of the $m = 0$ state for the Landau levels $n = 0, -1, -2$ and the impurity charge $\zeta = 1.4$.

Screening of charged impurity in a magnetic field

Poisson equation for the screened potential:

$$\sqrt{-\nabla_{2d}}V(\mathbf{x}) = -\frac{2\pi Ze^2}{\kappa}\delta(\mathbf{x}) - \frac{2\pi e^2}{\kappa}\int d^2\mathbf{y}\Pi(\mathbf{x}-\mathbf{y};\mu,B,\gamma)V(\mathbf{y}).$$

$$V(\mathbf{x}) = -\frac{Ze^2}{\kappa}\int_0^\infty dq \frac{qJ_0(q|\mathbf{x}|)}{q+\frac{2\pi e^2}{\kappa}\Pi(q;\mu,B,\gamma)}.$$

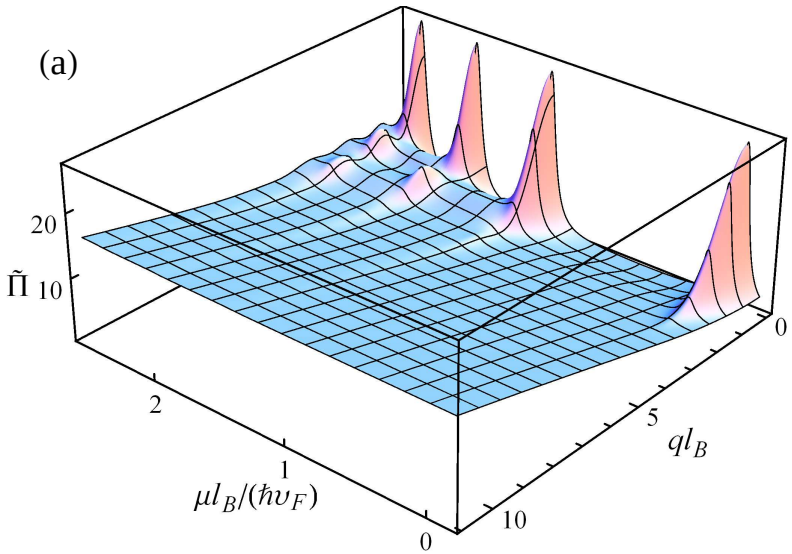

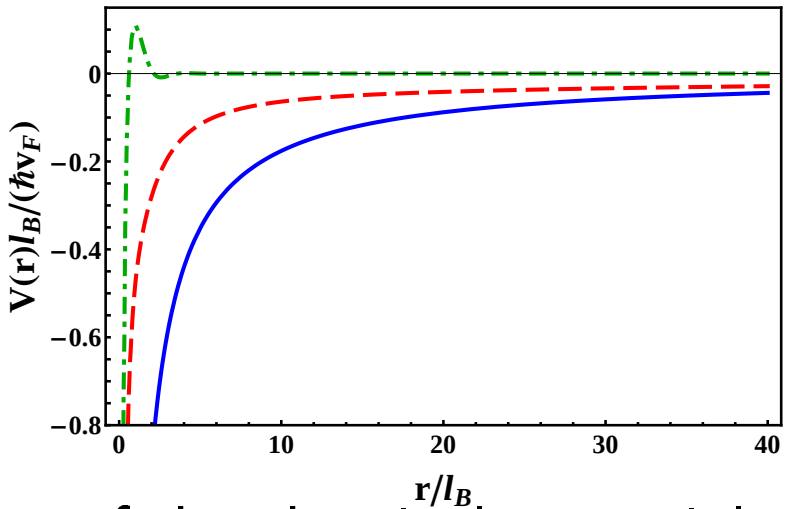

Polarization function as a function of the chemical potential and the wave vector (left panel) and the Coulomb potential (right panel).

Tuning the screening of charged impurity in a magnetic field

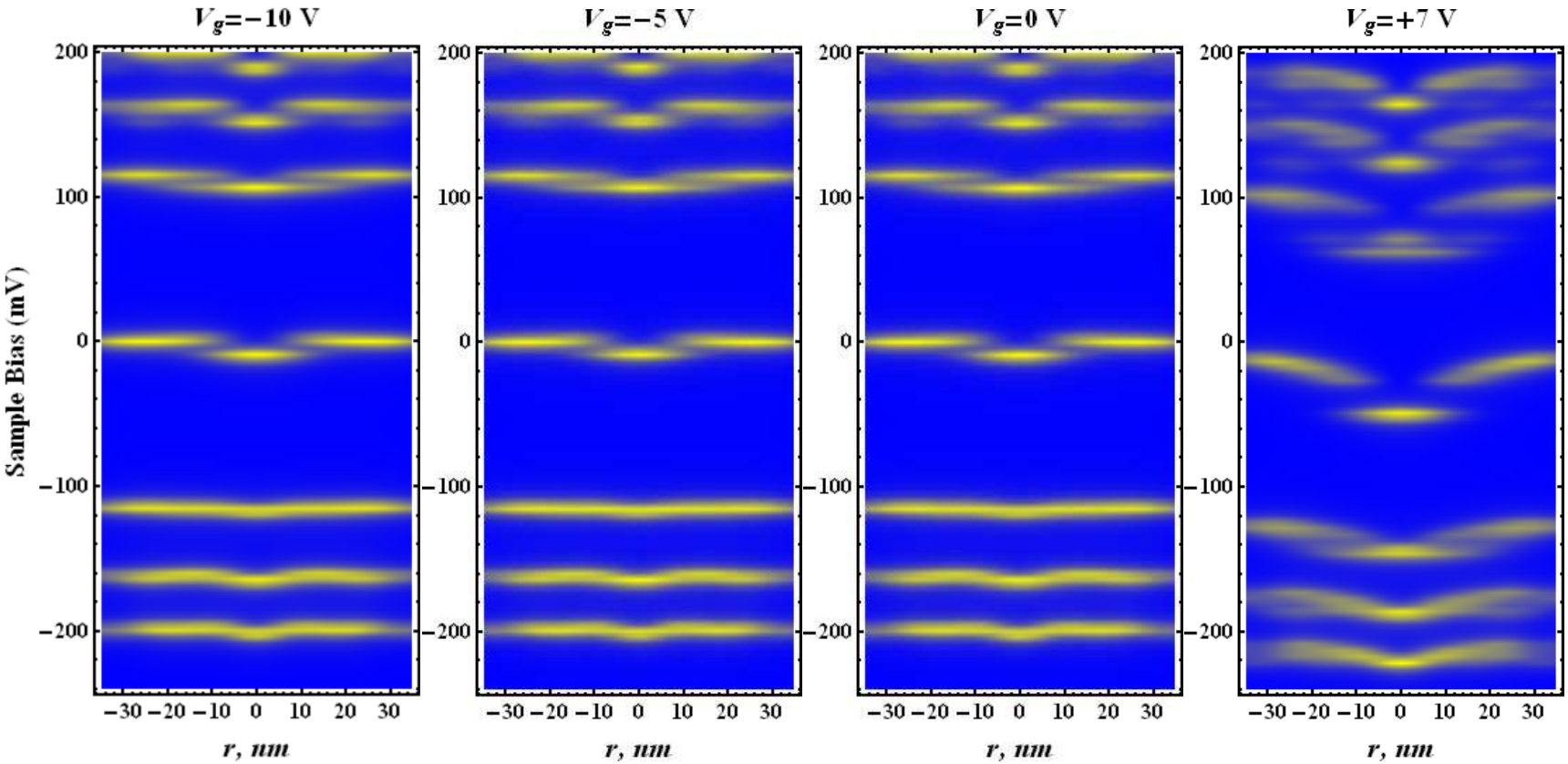

Theory: The local density of states plotted at four values of gate voltage and $B = 10$T - Sobol et al., Phys. Rev. B 94 (2016).

The strength of the impurity depends on the occupation of Landau-levels which can be controlled by a gate voltage.

Experiment: Luican-Mayer et al., PRL 112 (2014).

Simplified BCS model

$$\mathcal{L} = i\psi^\dagger_\alpha \frac{\partial}{\partial t}\psi_\alpha + \psi^\dagger_\alpha \left(\frac{\triangle}{2m} + E_F\right)\psi_\alpha + \frac{g}{2}\psi^\dagger_\alpha \psi^\dagger_\beta \psi_\beta \psi_\alpha,$$

$\alpha, \beta = \uparrow, \downarrow$ -spin, E_F - the Fermi energy. $U(1)$ symmetry: $\psi \to e^{i\theta}\psi$. BCS gap equation for the order parameter $\Delta = \langle \psi_\uparrow \psi_\downarrow \rangle$:

$$\Delta = g \int \frac{d^3p}{2(2\pi)^3} \frac{\Delta}{\sqrt{(p^2/2m - E_F)^2 + \Delta^2}}, \; |E - E_F| \leq \omega_D/2,$$

$E_F = p_F^2/2m$. Nontrivial solution $\Delta \neq 0$ exists at any small coupling g and finite E_F:

$$\Delta = \omega_D \exp\left(-\frac{2}{g\rho_F}\right), \; \rho(E) = \frac{m\sqrt{2mE}}{\pi^2} - \text{DOS}.$$

ρ_F - DOS at the Fermi surface. $U(1)$ symmetry is spontaneously broken. $E_F = 0$, the solution $\Delta \neq 0$ exists at $g > g_c = 2\pi^2/m^{3/2}\omega_D^{1/2}$!

Lagrangian of the NJL model (Phys. Rev. 122, 345 (1961))

$$\mathcal{L} = \bar{\Psi} i\gamma^\mu \partial_\mu \Psi + \frac{G}{2}\left[(\bar{\Psi}\Psi)^2 + (\bar{\Psi} i\gamma^5 \Psi)^2\right]$$

is invariant under ordinary and chiral gauge transformations

$$\Psi \to e^{i\alpha}\Psi, \quad \Psi \to e^{i\alpha\gamma^5}\Psi, \quad \Longrightarrow$$
$$\partial_\mu(\bar{\psi}\gamma^\mu\psi) = 0, \quad \partial_\mu(\bar{\psi}\gamma^\mu\gamma^5\psi) = 0.$$

Chiral symmetry forbids mass generation in perturbation theory. The self-consistent Hartree-Fock equation for the fermion propagator $G(p) = [\gamma^\mu p_\mu - m]^{-1}$,

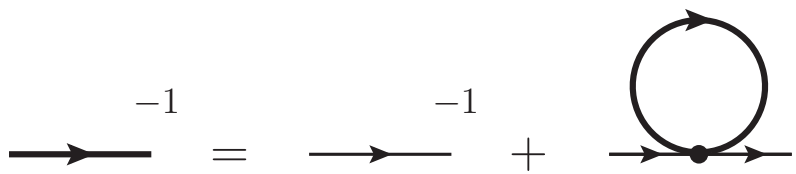

leads to the equation for dynamical mass (Λ is a cutoff):

$$\frac{1}{g} \equiv \frac{4\pi^2}{G\Lambda^2} = 1 - \frac{m^2}{\Lambda^2} \ln\left(1 + \frac{\Lambda^2}{m^2}\right).$$

It has a nontrivial solution for m if the coupling $G > G_c = 4\pi^2/\Lambda^2$ and the vacuum hosts a non-vanishing chiral condensate $\langle\bar{\Psi}\Psi\rangle \neq 0$.
Chiral symmetry is spontaneously broken.
DoS $\rho(E) \sim E^2$ for massless particles vanishes at $E = 0$ - the reason for G_c.
Under an external magnetic field the gap is generated at any coupling constant - magnetic catalysis:

$$m \simeq \sqrt{|eB|}\exp\left(-\frac{1}{2\rho_0 G}\right), \ \rho_0 = \frac{1}{V}\frac{dN}{dE}\Big|_{E=0} = \frac{|eB|}{4\pi^2} -$$

density of states at the lowest Landau level (compare with a superconducting gap).

The lowest Landau level with nonzero ρ_0 plays the role of the Fermi surface.

Mass generation in QED

$$\Delta = \omega_D \exp\left(-2/g\nu_F\right),$$

Bardeen-Cooper-Schrieffer (1957)

ω_D - Debye frequency,
g - electron-phonon coupling constant, ν_F - DOS on the Fermi surface.

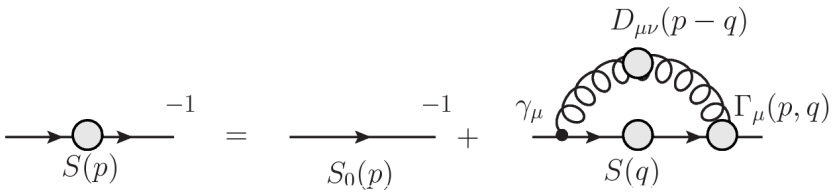

SD equation for the fermion propagator

$$S^{-1}(p) = A(p^2)\hat{p} - B(p^2),$$
$$B(0) \equiv m.$$

For the dynamical mass function $B(p^2)$ in the ladder approximation, one gets the nonlinear equation (70th-80th:Maskawa, Nakajima, Fukuda, Kugo, Kiev group, Filippov, Arbuzov, Atkinson)

$$B(p^2) = \frac{3\alpha}{4\pi}\int_0^{\Lambda^2} \frac{dk^2 B(k^2)}{k^2 + B^2(k^2)}\left(\frac{\theta(p^2-k^2)}{p^2} + \frac{\theta(k^2-p^2)}{k^2}\right)$$

Mass generation in QED

The linearized equation (with $B^2(k^2)$ in the denominator replaced by m^2) reduces to the Schrodinger-like equation in configuration space:

$$\left(-\Box - \frac{3\alpha/\pi}{r^2}\right)\Psi(r) = -m^2\Psi(r), \quad \Psi(r) = \int \frac{d^4k}{(2\pi)^4}\frac{e^{ikr}B(k^2)}{k^2+m^2},$$

with a singular potential $\sim 1/r^2$. Near the critical coupling:

$$m \simeq \Lambda \exp\left(-\frac{const}{\sqrt{\alpha-\alpha_c}}\right), \ \alpha_c \sim 1.$$

The solution combines features of a superconducting gap (non-analytical dependence on a coupling constant) and of the NJL gap (critical coupling).

Experimental search for strong coupling phase of QED:

GSI-Darmstadt in 80th (R.Peccei, Nature, 332, 492 (1988)).

Gap generation in graphene

The gap equation in the random phase approximation has the form:

$$\Delta(p) = \lambda \int_0^\Lambda \frac{dqq\Delta(q)\mathcal{K}(p,q)}{\sqrt{q^2 + (\Delta(q)/v_F)^2}}, \; \lambda = \frac{\alpha}{2(1+\pi\alpha/2)},$$

where $\alpha = e^2/(\hbar v_F) \approx 2.19$ is the "fine structure constant" for graphene, $v_F \approx 10^6 m/s$. The kernel

$$\mathcal{K}(p,q) = \frac{2}{\pi}\frac{1}{p+q}K\left(\frac{2\sqrt{pq}}{p+q}\right),$$

and K(x) is full elliptic integral of first kind. The nontrivial solution exists if the coupling $\lambda > 1/4$ ($\alpha > 1.62$):

$$\Delta(p=0) \simeq \Lambda v_F \exp\left(-\frac{\pi}{\sqrt{\lambda - 1/4}}\right).$$

The strong-coupling limit of graphene is an insulator.

Gap generation in graphene

In the random phase approximation with static vacuum polarization we find $\alpha_{crit} = 1.62$ is the quantum critical point of metal-insulator phase transition: Gamayun et al., PRB, 2010. When the dependence on the frequency is included

$$D(\omega, \mathbf{q}) = \frac{1}{|\mathbf{q}| + \Pi(\omega, \mathbf{q})}, \Pi(\omega, \mathbf{q}) = \frac{\pi e^2}{2\kappa} \frac{\mathbf{q}^2}{\sqrt{\hbar^2 v_F^2 \mathbf{q}^2 - \omega^2}},$$

the quantum critical point is $\alpha_{crit} = 0.92$. Monte-Carlo simulations give: $\alpha_{crit} = 1.11$ -Drut and Son, PRB, 2008, Drut abd Lahde, PRB, 2009, Hands and Strouthos, PRB, 2008.

No phase transition in real graphene: effective coupling $\alpha = e^2/\hbar v_F(q) < \alpha_{crit}$.

Magnetic catalysis in graphene

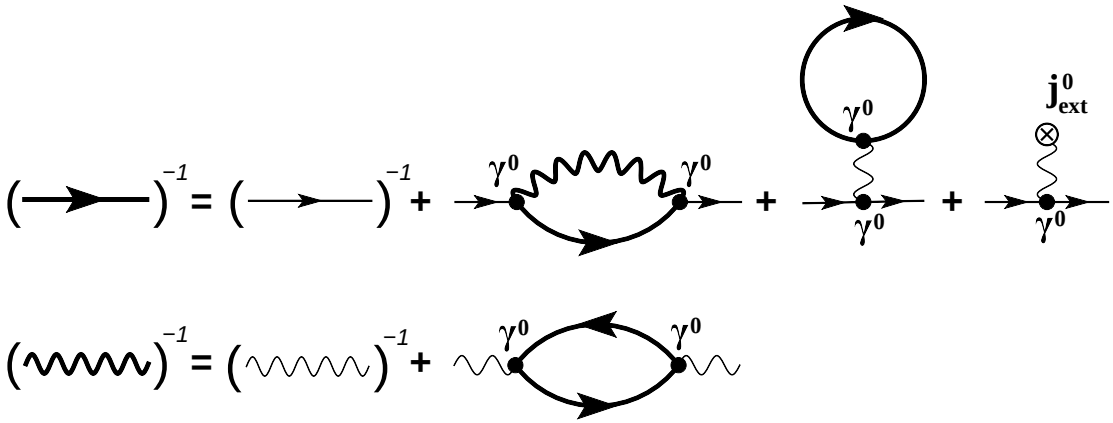

SD equation at finite B.

LLL approximation for the fermion propagator
$S(\omega) = [A(\omega)\gamma^0\omega - \Delta(\omega)]^{-1}$, $U(k)$ - Coulomb interaction,

$$S^{-1}(\omega) = S_0^{-1}(\omega) - ie^2 \int \frac{d\omega}{2\pi}\gamma^0 S(\omega)\gamma^0 \int \frac{d^2k}{(2\pi)^2} \exp\left(-\frac{k^2}{2eB}U(k)\right)$$

The solution for the gap $\Delta \sim \alpha_g\sqrt{eB}$ exists at any small α_g $(= e^2/\hbar v_F \kappa)$! [Gorbar, et al., PRB, 2002.]

Low-buckled Dirac materials

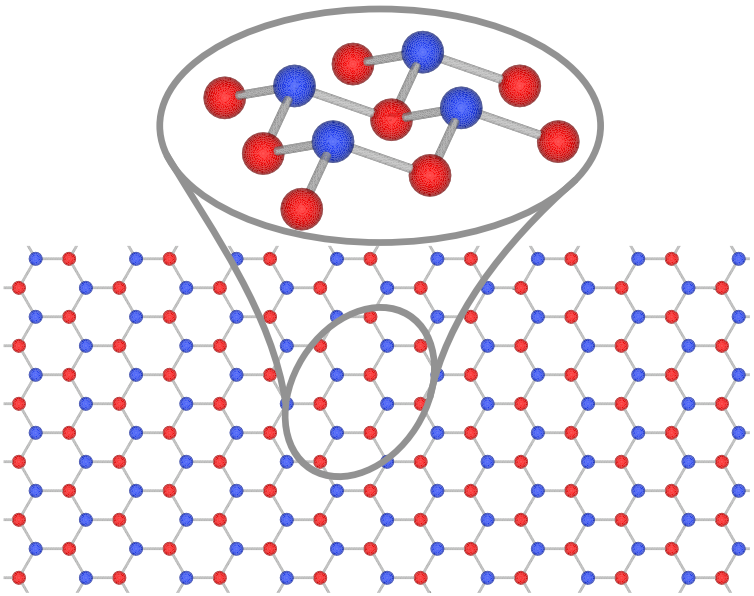

Silicene: vertical distance between sublattices $2d \approx 0.46$Å.
Lattice constant $a = 3.87$Å.
2D sheets of Ge, Sn, P and Pb atoms (the materials germanene, stanene and phosphorene).

Strong intrinsic spin-orbit interaction in contrast to graphene

$$H_{SO} = i\frac{\Delta_{SO}}{3\sqrt{3}} \sum_{\langle\langle i,j \rangle\rangle} c^{\dagger}_{i\sigma} (\boldsymbol{\nu}_{ij} \cdot \boldsymbol{\sigma})_{\sigma\sigma'} c_{j\sigma'}$$

with $\Delta_{SO} \sim 10\,\text{meV}$, $\nu^z_{ij} = \pm 1$.

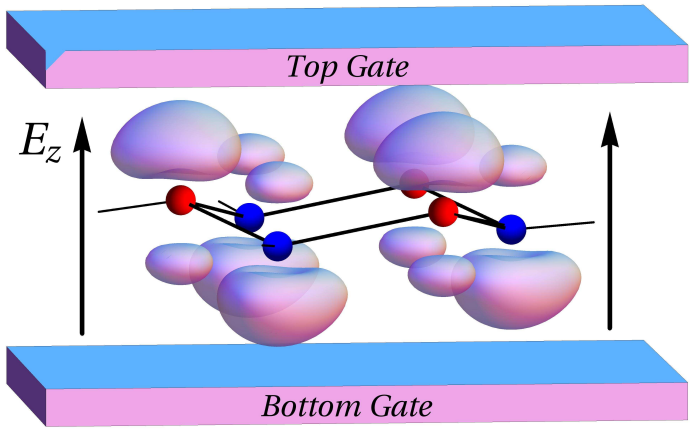

Perpendicular to the plane electric field E_z opens the tunable gap $\Delta_z = E_z d$.
Interplay of two gaps: Δ_{SO} and Δ_z.

Low-energy Hamiltonian for Silicene

$$\mathcal{H}_\xi = \sigma_0 \otimes [\hbar v_F(\xi k_x \tau_1 + k_y \tau_2) + \Delta_z \tau_3 - \mu \tau_0] - \xi \Delta_{\rm SO} \sigma_3 \otimes \tau_3,$$

$\boldsymbol{\tau}$ and $\boldsymbol{\sigma}$ – sublattice and spin; $\mathbf{k}$ is measured from the $\mathbf{K}_\xi$ points. $\Delta_{\rm SO}$ is due to the spin-orbit interaction. There is a spin $\sigma = \pm$, and valley $\xi = \pm$ dependent gap $\Delta_{\xi\sigma} = \Delta_z - \xi\sigma\Delta_{\rm SO}$. When $\Delta_{\xi\sigma} = 0$ we come back to graphene.

Time-reversal (TR) symmetry is unbroken.

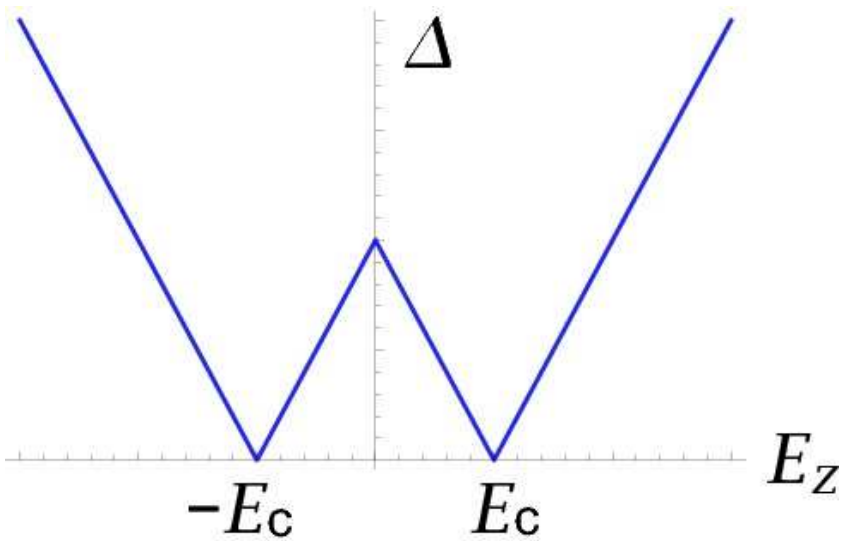

The band gap Δ as a function of the electric field E_z. The gap is open for $E_z \neq \pm E_c$, where silicene is an insulator. It is a topological insulator for $|E_z| < E_c$ (with edge states) and a band insulator for $|E_z| > E_c$.

Bilayer graphene

$$H = -\frac{1}{2m}\int d^2x \Psi^+_{Vs}(x) \begin{pmatrix} 0 & (\pi^\dagger)^2 \\ \pi^2 & 0 \end{pmatrix} \Psi_{Vs}(x) + \text{Zeeman}$$

+and Coulomb interactions, external electric field $E_\perp$

For n-layer graphene $\epsilon(\mathbf{p}) \sim |\mathbf{p}|^n$, $DOS(\epsilon) \sim \epsilon^{(2-n)/n}$,

$r_s = E_C/E_F \sim \rho^{(1-n)/2}$, Static polarization $\Pi(p) \sim p^{2-n}$.

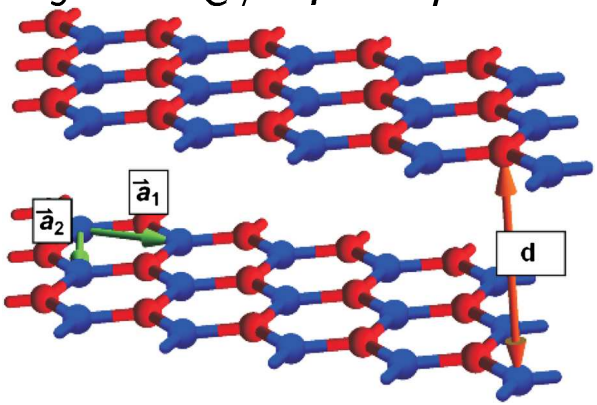

$$U(\omega, q) = \frac{2\pi e^2}{\kappa\left(q + (8\pi e^2/\kappa)\Pi(\omega, q)\right)},$$

$$\Pi(\omega, q) \simeq \frac{m \ln 4}{2\pi\sqrt{1 + \left(4 \ln 4 m\omega/\pi q^2\right)^2}}$$

Since for bilayer graphene, $n = 2$, DOS=const, the gap is generated at weak coupling (Nandkishore&Levitov, PRL, 2010):

$$\Delta \simeq (16me^4/\kappa^2\hbar^2) \exp\left(-12\pi^2/13\right) \approx \frac{2.6}{\kappa^2}\text{meV}.$$

THANK YOU FOR ATTENTION!